

Carbohydrate-based Polymer Brushes Prevent Viral Adsorption on Electrostatically Heterogeneous Interfaces

Ramya Kumar,^{†,⊥} Domenic Kratzer,[‡] Kenneth Cheng,^{¶,⊥} Julia Prisby,^{§,⊥} James

Sugai,^{||} William V. Giannobile,^{||} and Joerg Lahann^{*,†,¶,§,‡,⊥}

[†]*Department of Chemical Engineering, University of Michigan*

[‡]*Institute of Functional Interfaces, Karlsruhe Institute of Technology*

[¶]*Department of Material Science & Engineering, University of Michigan*

[§]*Department of Biomedical Engineering, University of Michigan*

^{||}*School of Dentistry, University of Michigan*

[⊥]*Biointerfaces Institute, University of Michigan*

E-mail: lahann@umich.edu

Abstract

Chemical heterogeneity on biomaterial surfaces can transform its interfacial properties, rendering nanoscale heterogeneity profoundly consequential during bioadhesion. To examine the role played by chemical heterogeneity in the adsorption of viruses on synthetic surfaces, we developed a range of novel coatings wherein a tunable mixture of electrostatic tethers for viral binding, and carbohydrate brushes, bearing pendant α -mannose, β -galactose or β -glucose groups, have been incorporated. We experimentally evaluated the effects of binding site density, brush composition and brush architecture on viral adsorption, with the goal of formulating design specifications for

virus-resistant coatings. We concluded that virus-coating interactions are shaped by the interplay between brush architecture and binding site density, after quantifying the adsorption of adenoviruses, influenza and fibrinogen on a library of carbohydrate brushes co-immobilized with different ratios of binding sites. These insights will be of utility in guiding the design of polymer coatings in realistic settings where they will be populated with defects.

Keywords

viral adsorption, glycopolymer brushes, QCM, influenza, adenovirus, bioadhesion, carbohydrate brushes

Main text

Interactions between biomaterial surfaces and biomolecules, bacteria or viruses instantaneously transform its surface, sometimes resulting in detrimental effects on its performance.¹ For instance, non-specific adsorption and denaturation of proteins on the surfaces of biomedical devices, such as insulin pumps, orthopedic devices and coronary stents, can adversely impact their function. Spatiotemporal control of DNA adhesion and transport in nanopore-based sequencing platforms still pose engineering challenges to which few solutions exist.² Beyond proteins and DNA, bacterial and viral adhesion pose even more complex challenges. Bacterial adsorption on catheters can trigger the formation of polymicrobial biofilm communities incorporating drug-resistant species.³ Adsorption of viruses to crops, soils and water purification membranes are significant problems in agriculture and environmental engineering.⁴ Recently, concern over the misuse of genetically modified influenza strains, Ebola and smallpox viruses as agents of biological warfare, has triggered investigations of virus-material interactions.⁵

Bioadhesion on synthetic materials has long been treated as a multifaceted problem,

encompassing material design parameters and biological variables.⁶ While we can seldom control biological variables such as the pH, ionic strength, the size, orientation and surface characteristics of the biological adsorbate, material properties can be specifically designed to elicit the desired outcome. In order to elucidate the complex relationships between interfacial properties, such as surface charge, hydrophilicity, roughness, topographical and nanomechanical features or chemical heterogeneity on the interfacial behavior of proteins, viruses or bacteria, model surfaces are required.⁷ Model surfaces, such as self-assembled monolayers (SAMs), possess tunable composition and structural features, thereby enabling systematic hypothesis testing and elucidation of relationships between material design features and adsorption outcomes, ultimately generating design guidelines and heuristics for engineered interfaces.^{8,9}

Although SAM-based model surfaces have been useful in evaluating the molecular mechanisms of protein adhesion, their practical utility has been limited by instability and incompatibility with polymer-based materials.^{10,11} Polymer brushes enjoy distinct advantages over SAMs since the substrate scope for polymer brushes is almost unlimited, and the instability associated with SAMs can be circumvented.¹² The advent of controlled radical polymerization techniques (CRP), such as surface-initiated atom transfer radical polymerization (SI-ATRP) have enabled the creation of tailored zwitterionic and carbohydrate polymer brushes.¹³

Researchers have investigated the effect of brush architecture on cell adhesion and migration,^{14,15} bacterial adhesion¹⁶ and non-specific protein adsorption,¹⁷ with the goal of identifying the optimal polymer brush design space. For instance the hemocompatibility of zwitterionic sulfobetaine¹⁸ and phosphorylcholine brushes¹⁹ was found to be strongly correlated with grafting density while sufficiently dense PEG layers were required to resist the adsorption of serum proteins.^{20,21} The relationships between bacterial adhesion and brush density,²² composition,²³ thickness,²⁴ and architectures²⁵ have been extensively examined. Despite methodological contrasts between these studies, they reached consensus on a few as-

pects: high brush densities are required to completely suppress protein, cellular and bacterial adhesion. Another finding is the critical role played by polymer conformation; vast differences in bioadhesion between highly stretched polymer brushes and mushroom-like polymer coils have been repeatedly observed. Model surfaces such as SAMs, peptidomimetic brushes²⁶ and PEG-PLL brushes²⁷⁻²⁹ have led to the formulation of design heuristics for surfaces with improved anti-fouling abilities and bacterial resistance. However, the majority of these studies have focused on protein adsorption, and to a limited extent bacterial adhesion, to the exclusion of adsorption processes involving viruses. Moreover, interfacial behavior of proteins is not helpful in predicting the adsorption levels of the other adsorbates. For instance, while some zwitterionic and glycopolymer brushes perform well against both bacteria and proteins, PEG brushes get colonized by bacteria despite repelling proteins. Recent studies have conclusively established that design rules for protein-resistant surfaces cannot be directly applied to prevent bacterial adhesion and vice versa.³⁰⁻³² Similar investigations probing the overlap in design criteria between virus-resistant surfaces and protein-resistant surfaces are lacking. Though methods to control viral attachment to synthetic surfaces are scarce, interactions between viruses and material surfaces have not yet been studied, except in the development of biosensors.^{33,34}

In this contribution, we have developed a novel library of polymer coatings wherein electrostatic tethers for virus binding are co-immobilized with well-defined carbohydrate brushes. We have examined the effects of brush architecture and binding site density on viral adhesion and determined design criteria for virus-resistant surfaces.

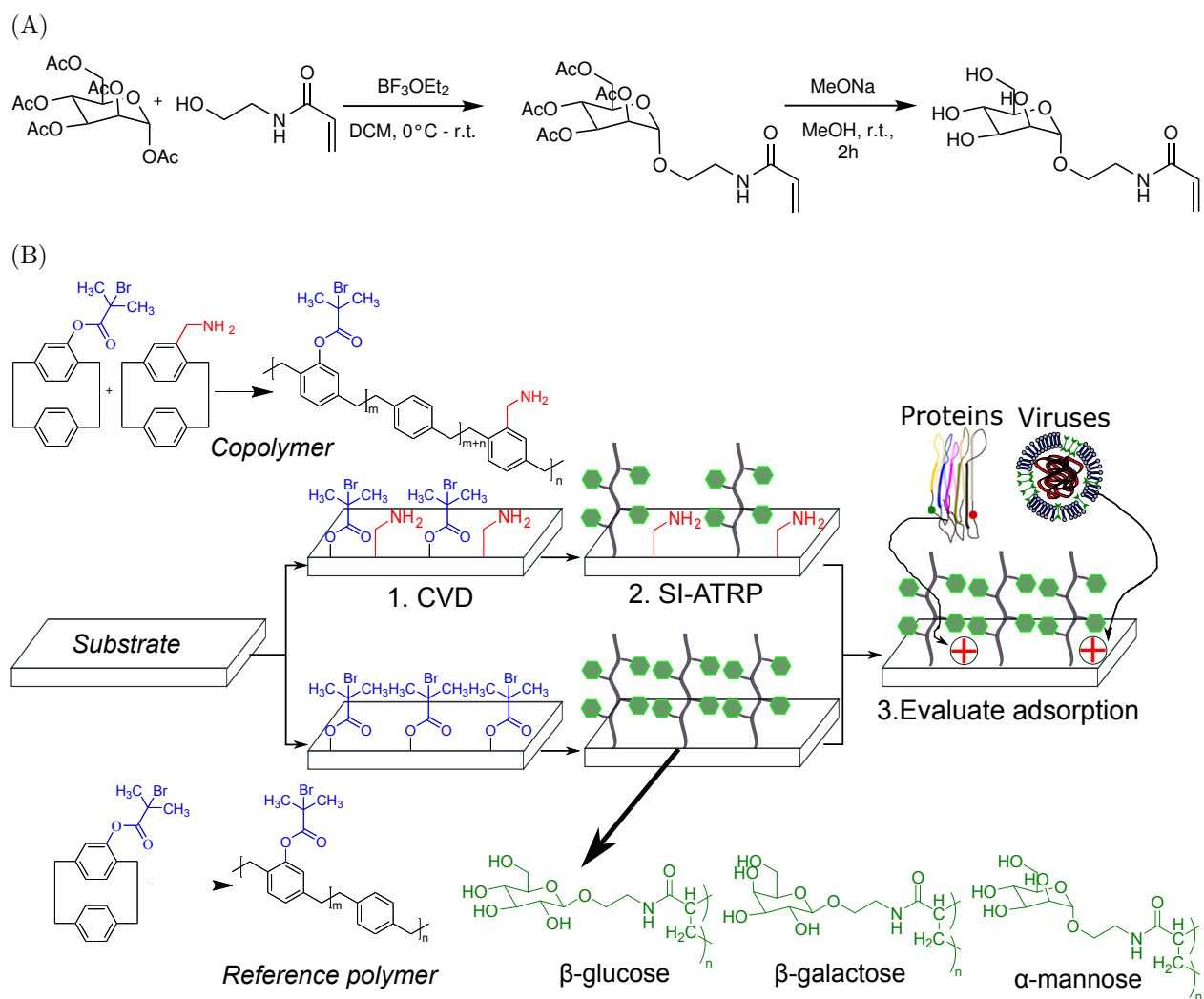
Chemical vapor deposition (CVD) polymerization is a versatile process that offers several benefits: not only is it solvent-free, pinhole-free and substrate-independent, this process produces reactive coatings with exceptional stability.³⁵ Our group has developed a library of [2,2]paracyclophanes, which allows multifunctional copolymer coatings of the desired composition to be accessed.³⁵ Using a custom-designed two-source CVD system, orthogonal co-presentation of SI-ATRP initiators with either alkynes, amines, activated esters, or alde-

hydes can be achieved.^{36,37} CVD copolymerization has enabled the preparation of binary copolymer gradients and subsequent co-immobilization of sugar molecules,³⁸ peptides and growth factors.³⁹ CVD copolymerization is unique in its capacity to produce surfaces that not only serve as model systems well-suited for basic research, but also bridge the gap between fundamental insights and technological translation.⁴⁰

While synthesizing polymer brushes, impurities, contaminants and processing limitations inevitably introduce defects on the surface, which often take the form of positively charged regions, compromising the ability of these brushes to resist bacterial and protein adsorption.⁴¹ The electrostatic forces originating from defects assume significance since most bacteria and viruses and many protein molecules bear a negative surface charge at physiological pH.^{42,43} Recognizing the importance of electrostatics in viral adsorption, we investigated the viral resistance of carbohydrate brushes when populated with positively charged defects. We combined CVD copolymerization and SI-ATRP to create a library of surfaces composed of positively charged binding sites and polymerization initiation sites for the growth of polymer brushes bearing carbohydrate residues (α -mannose, β -glucose and β -galactose). Binding sites introduced in the form of ionizable aminomethyl groups create positive charges that can influence viral and protein binding.

The synthetic route adopted to prepare carbohydrate functional monomers is displayed in Figure 1A. This synthetic strategy allows us to conjugate carbohydrates in their pyranose form to a polymerizable moiety, 2-hydroxy ethyl acrylamide, while still maintaining glycan bioactivity.⁴⁴ We opted for deprotection of the pyranose ring prior to polymerization instead of post-polymerization deprotection since the latter is seldom quantitative. Additionally, Yu and Kizhakkedathu⁴⁵ reported unsuccessful polymerization outcomes and incomplete deprotection when the protected monomer was employed.

After the monomer was synthesized, we proceeded to graft polymer brushes through SI-ATRP. First, substrates were functionalized with the ATRP initiator bearing bromosiobutryl groups via chemical vapor deposition polymerization.³⁶ Subsequently, poly(2'-acryl-



amidoethyl- α -d-mannopyranoside) brushes were grafted from the initiator coatings. Similar procedures for monomer synthesis and polymer brush growth were employed for preparing poly(2'-acrylamidoethyl- β -d-glucopyranoside) and poly(2'-acrylamidoethyl- β -d-galactopyranoside) brushes.

Our polymer coatings (Figure 1B) were prepared in two steps. First, the base layer was deposited on the substrates using CVD copolymerization and carbohydrate brushes were grafted subsequently. The base layer is a copolymer presenting both aminomethyl groups (AM) and ester bromide (EB) groups.

The ratio of AM to EB groups on the surface of the copolymer can be tuned and we have demonstrated compositional control in previous work.⁴⁶ We employed thermodynamic models (Figure S1 in SI) to predict how surface attributes impacted the degree of viral adsorption, and identified brush architecture and aminomethyl density as the key design variables. Our models predicted that viral adhesion would be promoted by AM groups and inhibited by the carbohydrate brushes.

Four different types of surfaces were synthesized (Figure 2A) using CVD (co)polymerization and SI-ATRP of α -mannose acrylamides. Fourier-transformed infrared (FTIR) spectroscopy was used to verify the presence of functional groups associated with each surface. The ester bromide groups were characterized by bands in the 1730 cm^{-1} and 1100 cm^{-1} regions, which correspond to C=O and C–O stretches. In addition to these two bands, the copolymer coatings also displayed a broad N–H band at 3400 cm^{-1} , signifying the presence of AM groups. After SI-ATRP, mannose brushes grafted from the copolymer and the initiator were analyzed using ellipsometry, FTIR spectroscopy (Figure 2B) as well as X-ray photoelectron spectroscopy (Figures S2 to S4 in SI). We observed the appearance of two new signals in the FTIR spectra upon grafting mannose polymers from the surface. The 3300 cm^{-1} band that is typical of the hydroxyl group and the N–C=O amide stretch at 1658 cm^{-1} , both of which confirm the formation of the mannose polymer brush.

We treated the reference and copolymer coatings to identical SI-ATRP conditions by

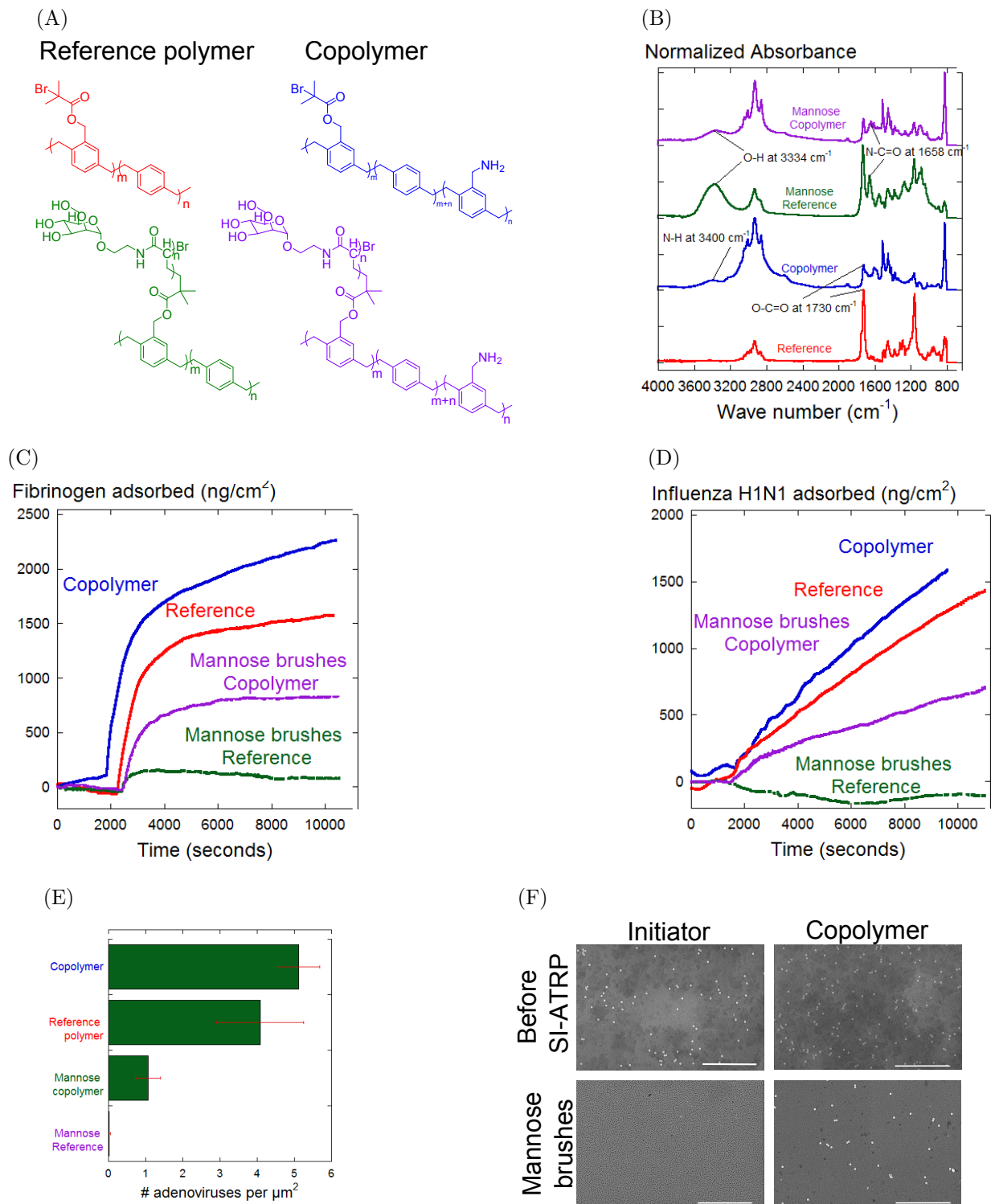


Figure 2: (A) Reference polymer, copolymer and mannose brushes grafted from each of these were studied. (B) FTIR confirms the chemical structures of these coatings. Effect of surface composition on the adsorption kinetics of (C) fibrinogen and (D) influenza H1N1 particles. In both (C) and (D), aminomethyl-containing surfaces promoted adsorption while the mannose brushes reduced adsorption levels. (E) Quantification of adenovirus attachment on surfaces. (F) Representative SEM images. Scale bar: 5 μm .

performing the polymerization in the same experiment. Ellipsometric measurements indicated that the mean thickness of mannose brushes grafted from the reference polymer and copolymer coatings were 17.4 nm and 1.4 nm respectively (Table S1 in SI). We attribute this difference in brush thickness to the reduced initiator density on the copolymer coatings, which results in the formation of dilutely bound polymer chains with lowered thickness as opposed to densely grafted and thicker brushes on reference polymer coatings.

Next we examined the effect of surface composition on the resistance to non-specific adsorption of fibrinogen, influenza H1N1 and adenoviruses. We measured fibrinogen adsorption on four different surfaces (reference and copolymer coatings, with and without α -mannose brushes) using a QCM. As seen in Figure 2C, the fibrinogen adsorption on the the copolymer and reference polymer (2000 and 1500 ng/cm² respectively) was greatly reduced when decorated with mannose brushes (750 and 50 ng/cm² respectively). This represents a 63% reduction in protein adsorption for the copolymer and a 97% reduction for the reference polymer. However protein adsorption was 15 times higher on copolymer coatings bearing mannose brushes compared to reference surfaces grafted to mannose brushes. Overall these results suggest that while the mannose brushes prevent fibrinogen deposition, the incorporation of AM groups promotes fibrinogen adsorption.

In the case of influenza H1N1 adsorption, we observed similar trends (Figure 2D). While a plateau value of around 500 ng/cm² was reached for the mannose brushes grafted from the copolymer, we found near-zero mass of adsorbed influenza on the reference surfaces with mannose brushes.

We also tested these four surfaces against adenoviruses (Figure 2E). The copolymer had the highest number of adenoviruses adsorbed per μm^2 , followed by the reference polymer and the mannose brushes grafted from the copolymer. In the absence of amino groups, the mannose brushes effectively inhibited adsorption of influenza virus.

Several experimental and theoretical studies have concluded that in addition to electrostatics, substrate roughness is also capable of inducing viral adhesion.⁴⁷⁻⁵⁰ In order to

ascertain that viral and protein adsorption was not confounded by topographical factors, we studied surface roughness using atomic force microscopy (Figure S5 in SI). Mean roughness values (R_a) below 2 nm were consistently observed on all CVD surfaces glucose, galactose and mannose brushes, indicating that all groups were smooth and topographical effects can be neglected.

The results from the fibrinogen, influenza and adenovirus studies prove that carbohydrate-functional brushes serve as potent barriers against viruses. Adsorption studies were repeated for β -glucose and β -galactose polymer brushes, with similar results (Figures S6 and S7 in the SI). We further concluded that viral adsorption was largely independent of the composition or stereochemistry of the carbohydrate brushes, because neither viral strain displayed specific affinities for any of the glycans employed.⁵¹

We then evaluated the effect of AM surface concentration and brush architecture on thin and sparse glucose brushes exemplified by four copolymer surfaces with varying amine concentrations.

The ratios between aminomethyl and ester bromide repeat units were varied in copolymer surfaces 1 through 4. As seen in Figure 3A, the carbonyl bands at 1730 cm^{-1} are prominent in copolymer 4, but not as intense in copolymers 1 and 2, indicating that 4 has the highest density of EB groups. Conversely, the C–H and N–H bands associated with the aminomethyl are most intense in copolymer 1 and their intensities decline steadily in copolymers 2, 3, 4, implying that copolymer 1 has the highest proportion of AM repeat units. These observations from FTIR studies were verified using XPS scans (Figure 3B) and the nitrogen content was highest in copolymer 1 and lowest in copolymer 4. Overall, FTIR and XPS results verified that copolymer coatings with a broad compositional range were synthesized.

Upon synthesizing and characterizing copolymer surfaces using CVD, glucose brushes were grafted from copolymers 1 through 4. All the copolymers underwent SI-ATRP in the same experimental run (reaction time: 1 hour) to ensure identical polymerization conditions. Ellipsometric characterization (Table 3C) of the resulting glucose coatings indicated

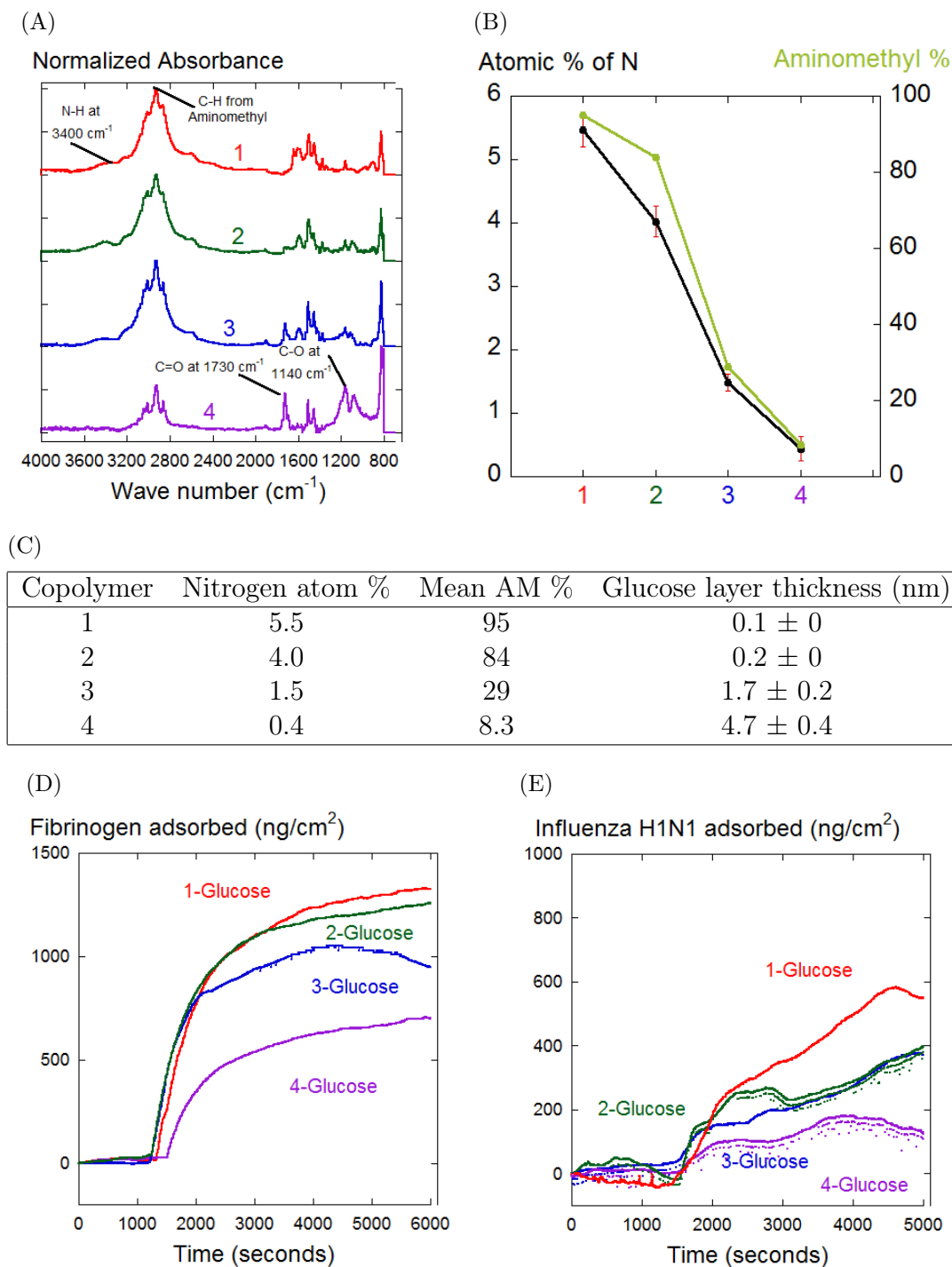


Figure 3: Four sets of copolymers (1-red, 2-green, 3-blue, 4-purple) with different concentrations of aminomethyl (AM) and ester bromide (EB) groups were prepared. (A) FTIR and (B) XPS measurements together verified that the AM concentration decreased progressively from copolymer 1 to 4. Conversely, the EB content increased as shown by the growing intensity of the carbonyl band. (C) Ellipsometric thicknesses of glucose polymers grafted from the copolymer coatings. QCM traces of (D) fibrinogen and (E) influenza indicate that the adsorption levels of both the protein and the virus particles are correlated with the AM density.

thicknesses ranged from under 1 nm for AM-rich copolymers 1 and 2 to nearly 5 nm for copolymer 4, which had the least AM groups and consequently the highest grafting density. These results agree with previous studies which reported that high grafting densities promote the formation of thicker brush-like polymers, while lower densities result in thin and sparse mushroom-like polymers.⁵²

Next, we performed QCM measurements of influenza and fibrinogen adsorption. For fibrinogen, we observed that glucose brushes grafted from copolymer 1 had the highest adsorbed mass of protein at around 1200 ng/cm² while those grafted from copolymer 4 displayed the least fibrinogen adsorption (650 ng/cm²) among the four surfaces compared. We observed similar trends for influenza adsorption, with 1-glucose and 4-glucose surfaces recording the highest and lowest influenza adsorption respectively.

For comparison, we also created a set of surfaces with higher glucose brush thicknesses and grafting densities. As seen in Figure 4A, though the FTIR bands representing the aminomethyl functionality are prominent in copolymer surface 5, the remaining surfaces in this set, copolymer 6, 7, 8 are mostly composed of EB repeat units. This finding is reinforced by XPS measurements (Figure 4B), where except for copolymer 5, whose composition reflects a 75%-25% split between the AM and EB components, respectively.

Again, glucose brushes were synthesized from these four surfaces under identical reaction conditions (reaction time: 24 hours). In Table 4C, we observed that though the glucose layer thickness is quite low for 5-glucose, the remaining samples (6,7 and 8) recorded thickness values ranging from 3-5 nm. We attribute this contrast between copolymer 5 and the other copolymers to the higher AM content in 5 and denser distribution of ATRP-initiating EB moieties in copolymers 6 through 8. Additionally, the increase in reaction time compared to the first set of surfaces (24 hours as opposed to 1 hour) resulted in higher degree of polymerization.

Next, we evaluated the interactions between glucose brushes and fibrinogen using QCM measurements. In the 5-glucose surfaces, we detected a small decrease in the measured fre-

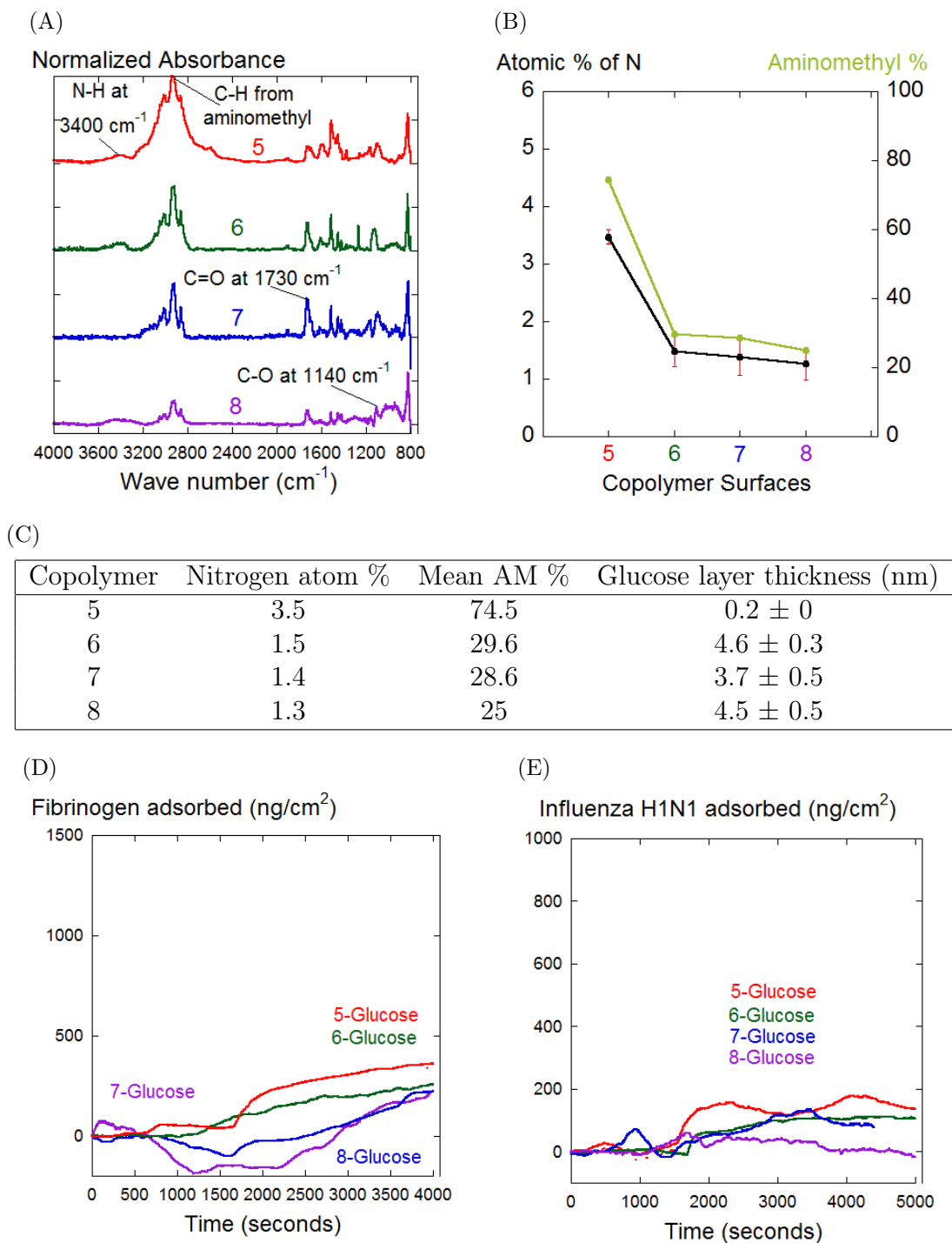


Figure 4: Four sets of copolymer coatings (5-red, 6-green, 7-blue, 8-purple) with different ratios of aminomethyl (AM) and ester bromide (EB) groups were synthesized and differences in adsorption evaluated. (A) FTIR spectra and (B) X-ray photoelectron spectroscopy (XPS) were jointly employed to assess variations in AM content. Subsequently, glucose polymer chains (ellipsometric thicknesses tabulated) were grafted from these surfaces using SI-ATRP. The adsorption kinetics of (D) fibrinogen and (E) influenza H1N1 on glucose chains grown from copolymers were studied using QCM. For both fibrinogen and influenza, adsorbed masses were near baseline levels, indicating that the glucose layers prevented non-specific protein and viral adsorption.

quency upon the introduction of fibrinogen at 1800 seconds, indicating that only a low quantity of protein had been adsorbed. As for the rest, the deviation of frequency measurements from baseline levels was even smaller, and in two cases (7-glucose and 8-glucose), the frequency readings could not be distinguished from the baselines. Similar results were obtained when we assessed influenza H1N1 adsorption on these surfaces, with barely discernible decreases in frequency being recorded upon the injection of the influenza suspension. Overall, we concluded that both non-specific protein and viral adsorption levels were minimal (100-200 ng/cm²) in the second set of copolymers (5 to 8).

We note that the adsorption profiles were independent of binding site density in Figure 4 but varied with AM density in Figure 3. This suggests that AM density alone cannot influence adsorption outcomes. Rather, it is apparent that adsorption behavior is shaped by the complex interplay between binding site density and polymer conformation.

In this study, we developed an interfacial approach towards incorporating carbohydrate brushes of tailored composition and architecture as well as AM groups, which served as binding sites promoting viral adhesion. Employing a combination of CVD copolymerization and surface-initiated atom transfer radical polymerization, we synthesized multifunctional polymer coatings where the carbohydrate brushes and positively charged binding sites were co-immobilized in the desired ratio. We concluded that the adsorption of viruses is a complex function of AM concentration and carbohydrate brush architecture. By allowing the carbohydrate brushes to grow to their maximum extent and attain brush thicknesses around 3-5 nm, low levels of protein and viral adsorption were achieved, even when the AM proportion was as high as 25-30%. When carbohydrate polymer chains were sufficiently thick and dense, the resulting steric and hydration repulsion effectively blocked the virus from interacting with the positively charged affinity sites. Virus-resistant coatings retained their barrier-like properties if the surrounding carbohydrate chains suppressed attractive interactions offered by the defects.

Acknowledgement

We acknowledge the Defense Threat Reduction Agency (DTRA) for funding provided through grant HDTRA1-12-1-0039 as a part of the interfacial dynamics and reactivity program. We gratefully acknowledge the Engineering Research Centers Program of the National Science Foundation for funding provided through award EEC-1647837. R.K. gratefully acknowledges Rackham Graduate School for providing financial support through the Rackham Predoctoral Fellowship.

Supporting Information Available

The following files are available free of charge.

- virussupinfo.pdf : Modeling results, ellipsometry, FTIR, contact angle, surface roughness, XPS, experimental procedures.

References

- (1) Palacio, M. L. B.; Bhushan, B. Bioadhesion: a review of concepts and applications. *Philosophical Transactions of the Royal Society A: Mathematical, Physical and Engineering Sciences* **2012**, *370*, 2321–2347.
- (2) Wang, D.; Harrer, S.; Luan, B.; Stolovitzky, G.; Peng, H.; Afzali-Ardakani, A. Regulating the Transport of DNA through Biofriendly Nanochannels in a Thin Solid Membrane. *Scientific Reports* **2015**, *4*, 3985.
- (3) Campoccia, D.; Montanaro, L.; Arciola, C. R. The significance of infection related to orthopedic devices and issues of antibiotic resistance. *Biomaterials* **2006**, *27*, 2331–2339.

- (4) Seidel, M.; Jurzik, L.; Brettar, I.; Höfle, M. G.; Griebler, C. Microbial and viral pathogens in freshwater: current research aspects studied in Germany. *Environmental Earth Sciences* **2016**, *75*.
- (5) Shoham, D. Influenza type A virus: an outstandingly protean pathogen and a potent modular weapon. *Critical reviews in microbiology* **2013**, *39*, 123–138.
- (6) Katsikogianni, M.; Missirlis, Y. F. Concise review of mechanisms of bacterial adhesion to biomaterials and of techniques used in estimating bacteria-material interactions. *European Cells and Materials* **2004**, *8*, 37–57.
- (7) Kevin L . Prime and George M . Whitesides, Self-Assembled Organic Monolayers : Model Systems for Studying Adsorption of Proteins at Surfaces. *Science (New York, N.Y.)* **2009**, *252*, 1164–1167.
- (8) Ostuni, E.; Chapman, R. G.; Liang, M. N.; Meluleni, G.; Pier, G.; Ingber, D. E.; Whitesides, G. M. Self-Assembled Monolayers That Resist the Adsorption of Cells. *Langmuir* **2001**, *17*, 6336–6343.
- (9) Mrksich, M.; Whitesides, G. M. Using Self-Assembled Monolayers to Understand the Interactions of Man-made Surfaces with Proteins and Cells. *Annual Review of Biophysics and Biomolecular Structure* **1996**, *25*, 55–78.
- (10) Srisombat, L.; Jamison, A. C.; Lee, T. R. Stability: A key issue for self-assembled monolayers on gold as thin-film coatings and nanoparticle protectants. *Colloids and Surfaces A: Physicochemical and Engineering Aspects* **2011**, *390*, 1–19.
- (11) Flynn, N. T.; Tran, T. N. T.; Cima, M. J.; Langer, R. Long-term stability of self-assembled monolayers in biological media. *Langmuir* **2003**, *19*, 10909–10915.
- (12) Hucknall, A.; Rangarajan, S.; Chilkoti, A. In Pursuit of Zero: Polymer Brushes that Resist the Adsorption of Proteins. *Advanced Materials* **2009**, *21*, 2441–2446.

- (13) Barbey, R.; Lavanant, L.; Paripovic, D.; Schüwer, N.; Sugnaux, C.; Tugulu, S.; Klok, H.-A. Polymer brushes via surface-initiated controlled radical polymerization: synthesis, characterization, properties, and applications. *Chemical reviews* **2009**, *109*, 5437–527.
- (14) Singh, N.; Cui, X.; Boland, T.; Husson, S. M. The role of independently variable grafting density and layer thickness of polymer nanolayers on peptide adsorption and cell adhesion. *Biomaterials* **2007**, *28*, 763–771.
- (15) Wu, J.; Mao, Z.; Gao, C. Controlling the migration behaviors of vascular smooth muscle cells by methoxy poly(ethylene glycol) brushes of different molecular weight and density. *Biomaterials* **2012**, *33*, 810–820.
- (16) Cringus-Fundeanu, I.; Luijten, J.; Van Der Mei, H. C.; Busscher, H. J.; Schouten, A. J. Synthesis and characterization of surface-grafted polyacrylamide brushes and their inhibition of microbial adhesion. *Langmuir* **2007**, *23*, 5120–5126.
- (17) Choi, S.; Choi, B. C.; Xue, C.; Leckband, D. Protein adsorption mechanisms determine the efficiency of thermally controlled cell adhesion on poly(N -isopropyl acrylamide) brushes. *Biomacromolecules* **2013**, *14*, 92–100.
- (18) Chang, Y.; Chang, Y.; Higuchi, A.; Shih, Y. J.; Li, P. T.; Chen, W. Y.; Tsai, E. M.; Hsiue, G. H. Bioadhesive control of plasma proteins and blood cells from umbilical cord blood onto the interface grafted with zwitterionic polymer brushes. *Langmuir* **2012**, *28*, 4309–4317.
- (19) Lu, C. Y.; Zhou, N. L.; Xiao, Y. H.; Tang, Y. D.; Jin, S. X.; Wu, Y.; Zhang, J.; Shen, J. Surface grafting density analysis of high anti-clotting PU-Si-g-P(MPC) films. *Applied Surface Science* **2012**, *258*, 3920–3926.
- (20) Emilsson, G.; Schoch, R. L.; Feuz, L.; Höök, F.; Lim, R. Y.; Dahlin, A. B. Strongly stretched protein resistant poly(ethylene glycol) brushes prepared by grafting-to. *ACS Applied Materials and Interfaces* **2015**, *7*, 7505–7515.

- (21) Faulón Marruecos, D.; Kastantin, M.; Schwartz, D. K.; Kaar, J. L. Dense Poly(ethylene glycol) Brushes Reduce Adsorption and Stabilize the Unfolded Conformation of Fibronectin. *Biomacromolecules* **2016**, *17*, 1017–1025.
- (22) Ibanescu, S. A.; Nowakowska, J.; Khanna, N.; Landmann, R.; Klok, H. A. Effects of Grafting Density and Film Thickness on the Adhesion of *Staphylococcus epidermidis* to Poly(2-hydroxy ethyl methacrylate) and Poly(poly(ethylene glycol)methacrylate) Brushes. *Macromolecular Bioscience* **2016**, *16*, 676–685.
- (23) Yu, K.; Lo, J. C.; Mei, Y.; Haney, E. F.; Siren, E.; Kalathottukaren, M. T.; Hancock, R. E.; Lange, D.; Kizhakkedathu, J. N. Toward Infection-Resistant Surfaces: Achieving High Antimicrobial Peptide Potency by Modulating the Functionality of Polymer Brush and Peptide. *ACS Applied Materials and Interfaces* **2015**, *7*, 28591–28605.
- (24) Yadav, V.; Jaimes-Lizcano, Y. A.; Dewangan, N. K.; Park, N.; Li, T.-H.; Robertson, M. L.; Conrad, J. C. Tuning Bacterial Attachment and Detachment via the Thickness and Dispersity of a pH-Responsive Polymer Brush. *ACS Applied Materials & Interfaces* **2017**, *9*, 44900–44910, PMID: 29215264.
- (25) Pidhatika, B.; Möller, J.; Benetti, E. M.; Konradi, R.; Rakhmatullina, E.; Mühlbach, A.; Zimmermann, R.; Werner, C.; Vogel, V.; Textor, M. The role of the interplay between polymer architecture and bacterial surface properties on the microbial adhesion to polyoxazoline-based ultrathin films. *Biomaterials* **2010**, *31*, 9462–9472.
- (26) Lau, K. H. A.; Sileika, T. S.; Park, S. H.; Sousa, A. M. L.; Burch, P.; Szleifer, I.; Messersmith, P. B. Molecular Design of Antifouling Polymer Brushes Using Sequence-Specific Peptoids. *Advanced Materials Interfaces* **2015**, *2*, 1–10.
- (27) Kalasin, S.; Dabkowski, J.; Nüsslein, K.; Santore, M. M. The role of nano-scale hetero-

geneous electrostatic interactions in initial bacterial adhesion from flow: A case study with *Staphylococcus aureus*. *Colloids and Surfaces B: Biointerfaces* **2010**, *76*, 489–495.

- (28) Gon, S.; Santore, M. M. Single Component and Selective Competitive Protein Adsorption in a Patchy Polymer Brush: Opposition between Steric Repulsions and Electrostatic Attractions. *Langmuir* **2011**, *27*, 1487–1493.
- (29) Gon, S.; Kumar, K.-N.; Nüsslein, K.; Santore, M. M. How Bacteria Adhere to Brushy PEG Surfaces: Clinging to Flaws and Compressing the Brush. *Macromolecules* **2012**, *45*, 8373–8381.
- (30) Cheng, G.; Zhang, Z.; Chen, S.; Bryers, J. D.; Jiang, S. Inhibition of bacterial adhesion and biofilm formation on zwitterionic surfaces. *Biomaterials* **2007**, *28*, 4192–4199.
- (31) Wang, Y.; Narain, R.; Liu, Y. Study of Bacterial Adhesion on Different Glycopolymer Surfaces by Quartz Crystal Microbalance with Dissipation. *Langmuir* **2014**, *30*, 7377–7387.
- (32) Wei, J.; Ravn, D. B.; Gram, L.; Kingshott, P. Stainless steel modified with poly(ethylene glycol) can prevent protein adsorption but not bacterial adhesion. *Colloids and Surfaces B: Biointerfaces* **2003**, *32*, 275–291.
- (33) Madeleine, R. *Polymer and Biopolymer Brushes*; Wiley-Blackwell, 2017; Chapter 19, pp 515–556.
- (34) Riedel, T.; Rodriguez-Emmenegger, C.; de los Santos Pereira, A.; Bedajankova, A.; Jinoch, P.; Boltovets, P. M.; Brynda, E. Diagnosis of Epstein-Barr virus infection in clinical serum samples by an SPR biosensor assay. *Biosensors and Bioelectronics* **2014**, *55*, 278 – 284.
- (35) Deng, X.; Lahann, J. Orthogonal surface functionalization through bioactive vapor-based polymer coatings. *Journal of Applied Polymer Science* **2014**, *131*.

- (36) Jiang, X.; Chen, H.-Y.; Galvan, G.; Yoshida, M.; Lahann, J. Vapor-Based Initiator Coatings for Atom Transfer Radical Polymerization. *Advanced Functional Materials* **2008**, *18*, 27–35.
- (37) Nandivada, H.; Chen, H.-Y.; Bondarenko, L.; Lahann, J. Reactive Polymer Coatings that “Click”. *Angewandte Chemie (International ed. in English)* **2006**, *45*, 3360–3363.
- (38) Bally, F.; Cheng, K.; Nandivada, H.; Deng, X.; Ross, A. M.; Panades, A.; Lahann, J. Co-immobilization of biomolecules on ultrathin reactive chemical vapor deposition coatings using multiple click chemistry strategies. *ACS applied materials & interfaces* **2013**, *5*, 9262–8.
- (39) Deng, X.; Lahann, J. A generic strategy for co-presentation of heparin-binding growth factors based on CVD polymerization. *Macromolecular rapid communications* **2012**, *33*, 1459–65.
- (40) Elkasabi, B. Y.; Chen, H.-y.; Lahann, J. Multipotent Polymer Coatings Based on Chemical Vapor Deposition Copolymerization. *Advanced Materials* **2006**, *18*, 1521–1526.
- (41) Hori, K.; Matsumoto, S. Bacterial adhesion: From mechanism to control. *Biochemical Engineering Journal* **2010**, *48*, 424–434.
- (42) Michen, B.; Graule, T. Isoelectric points of viruses. *Journal of Applied Microbiology* **2010**, *109*, 388–397.
- (43) Norde, W.; Lyklema, J. Protein adsorption and bacterial adhesion to solid surfaces: A colloid-chemical approach. *Colloids and Surfaces* **1989**, *38*, 1–13.
- (44) Wilkins, L. E.; Phillips, D. J.; Deller, R. C.; Davies, G.-L.; Gibson, M. I. Synthesis and characterisation of glucose-functional glycopolymers and gold nanoparticles: study of their potential interactions with ovine red blood cells. *Carbohydrate Research* **2015**, *405*, 47 – 54, Glyconanomaterials.

- (45) Yu, K.; Kizhakkedathu, J. N. Synthesis of Functional Polymer Brushes Containing Carbohydrate Residues in the Pyranose Form and Their Specific and Nonspecific Interactions with Proteins. *Biomacromolecules* **2010**, *11*, 3073–3085, PMID: 20954736.
- (46) Kumar, R.; Kopyeva, I.; Cheng, K.; Liu, K.; Lahann, J. Examining Nanoparticle Adsorption on Electrostatically “Patchy” Glycopolymer Brushes Using Real-Time ζ -Potential Measurements. *Langmuir* **2017**, *33*, 6322–6332, PMID: 28574709.
- (47) Hermansson, M. The DLVO theory in microbial adhesion. *Colloids and Surfaces B: Biointerfaces* **1999**, *14*, 105 – 119.
- (48) Lu, L.; Ku, K.-M.; Palma-Salgado, S. P.; Storm, A. P.; Feng, H.; Juvik, J. A.; Nguyen, T. H. Influence of Epicuticular Physicochemical Properties on Porcine Rotavirus Adsorption to 24 Leafy Green Vegetables and Tomatoes. *PLOS ONE* **2015**, *10*, 1–21.
- (49) Dika, C.; Ly-Chatain, M.; Francius, G.; Duval, J.; Gantzer, C. Non-DLVO adhesion of F-specific RNA bacteriophages to abiotic surfaces: Importance of surface roughness, hydrophobic and electrostatic interactions. *Colloids and Surfaces A: Physicochemical and Engineering Aspects* **2013**, *435*, 178 – 187, Special Issue : IAP 2012.
- (50) Armanious, A.; Aeppli, M.; Jacak, R.; Refardt, D.; Sigstam, T.; Kohn, T.; Sander, M. Viruses at Solid–Water Interfaces: A Systematic Assessment of Interactions Driving Adsorption. *Environmental Science & Technology* **2016**, *50*, 732–743, PMID: 26636722.
- (51) Van Breedam, W.; Pöhlmann, S.; Favoreel, H. W.; de Groot, R. J.; Nauwynck, H. J. Bitter-sweet symphony: glycan-lectin interactions in virus biology. *FEMS Microbiology Reviews* **2014**, *38*, 598–632.
- (52) Zou, Y.; Rossi, N. A.; Kizhakkedathu, J. N.; Brooks, D. E. Barrier capacity of hydrophilic polymer brushes to prevent hydrophobic interactions: Effect of graft density and hydrophilicity. *Macromolecules* **2009**, *42*, 4817–4828.

Table of contents entry:

A tunable coating comprising non-fouling carbohydrate brushes and electrostatic binding sites for viruses has been employed to study the relationship between surface design parameters and viral adsorption. Ultimately, brush architecture determines whether the binding sites are exposed to, or shielded from viruses. These insights will guide the design of polymer coatings that can resist viral binding despite being populated with defects.

Graphical TOC Entry

